EXTENSIVE MAPPING OF BERING SEA AND GULF OF ALASKA COASTAL CHANGE BY LANDSAT TIME SERIES TREND ANALYSIS, 1972–2013

PHASE 1: FEASIBILITY ANALYSIS

Prepared for
Western Alaska Landscape Conservation Cooperative
Anchorage, Alaska

Prepared by
ABR, Inc.–Environmental Reseach & Services
Fairbanks, Alaska

EXTENSIVE MAPPING OF BERING SEA AND GULF OF ALASKA COASTAL CHANGE BY LANDSAT TIME SERIES TREND ANALYSIS, 1972–2013

PHASE I: FEASIBILITY ANALYSIS

FINAL REPORT

Prepared by:
Matthew J. Macander
Christopher S. Swingley
ABR, Inc.—Enviromental Research & Services
Fairbanks, Alaska

Prepared for:
Western Alaska Landscape Conservation Cooperative
US Fish and Wildlife Service
Anchorage, Alaska

May 2013

This report was produced under U.S. Fish and Wildlife Service Award Number F13AC00156 on behalf of the Western Alaska LCC. The views and conclusions contained in this document are those of the authors and should not be interpreted as representing the opinions or policies of the U.S. Government. Mention of trade names or commercial products does not constitute their endorsement by the U.S. Government.

ACKNOWLEDGMENTS

We thank Karen Murphy and Joel Reynolds with the Western Alaska Landscape Conservation Cooperative for support and management of this project. Review of the report was provided by Tako Raynolds with the University of Alaska Fairbanks and ABR, Inc.; Joel Reynolds and Karen Murphy with the Western Alaska Landscape Conservation Cooperative; and Craig Ely with the United States Geological Survey.

For more information, please contact:

Matt Macander, ABR, Inc.
907-455-6777, ext 112
mmacander@abrinc.com

Cover photo: A portion of the Landsat time-series for tile AKH063V16, which includes parts of the Baldwin Peninsula, Hotham Inlet, and Kobuk River Delta in northwest Alaska.

TABLE OF CONTENTS

TABLES

FIGURES

INTRODUCTION

The landscape-scale effects of coastal storms on Alaska's Bering Sea coast include coastal erosion, migration of spits and barrier islands, breaching of coastal lakes and lagoons, and inundation and salt-kill of vegetation. In areas experiencing moderate to large effects, changes can be mapped by analyzing trends in time series of Landsat imagery from the MultiSpectral Scanner (MSS), Thematic Mapper (TM) and Enhanced Thematic Mapper (ETM+). The archive of Landsat imagery covers the time period 1972–present. Regression analysis will identify areas with significant changes in coastal features across the study period.

Extensive mapping of coastal change along the Bering Sea and Gulf of Alaska coasts will provide important baseline information on the distribution and magnitude of landscape changes over the past 41 years (1972–2013). The extent of change to the coastline and to coastal features, such as spits, barrier islands, estuaries, tidal guts and lagoons, is known to be substantial in some areas along the Bering Sea coast (e.g., portions of the Yukon–Kuskokwim Delta), although the extent of change along the full Bering Sea coast is not well documented. With this analysis, the extent of recent habitat loss can be summarized for different land ownerships or other units. Hotspots of change identified by the wide coverage of the mapping proposed in this study will provide guidance on selecting areas for monitoring or for more intensive research (e.g., terrain sensitivity analysis).

The primary objective of the overall study is to map the distribution and extent of areas with significant spectral change along the Bering Sea coast and Gulf of Alaska coast, within the boundary of the Western Alaska LCC. The changes will be classified and labeled to identify land-cover transitions (e.g., tundra to water, barrens to water, tundra to barrens, and water to barrens). In many cases, we expect to be able to attribute the changes to particular coastal change mechanisms.

For this feasibility analysis (Phase I) the objectives are 1) to assess the availability (spatial and temporal) of suitable Landsat imagery over the study area; and 2) provide examples of the change detection methods for demonstration sites in the study area using MSS imagery and TM/ETM+ imagery. Based on the results of the feasibility analysis, the Western Alaska LCC

will decide how much of the coastline within their boundary to process using a Landsat change detection approach.

STUDY AREA

The *Bering Sea* study area includes the entire Bering Sea coast within the bounds of the Western Alaska Landscape Conservation Cooperative (WALCC, Figure 1, Map A). This area extends from Kotzebue to Sennet Point (at the west end of Unimak Island); the Seward Peninsula, Yukon–Kuskokwim Delta, the north coast of the Alaska Peninsula, and Nunivak Island also are included. Approximately 11,569 km of "coastline" are included within this study area, based on the Alaska 1:63,360 coastline map produced by the Alaska Department of Natural Resources in 1998. This total length includes outer and inner portions of barrier islands and various portions of river mouth channels. A total of 201 30-km Landsat tiles (defined under Methods: Preprocessing below) include portions of the Bering Sea coast in the study area.

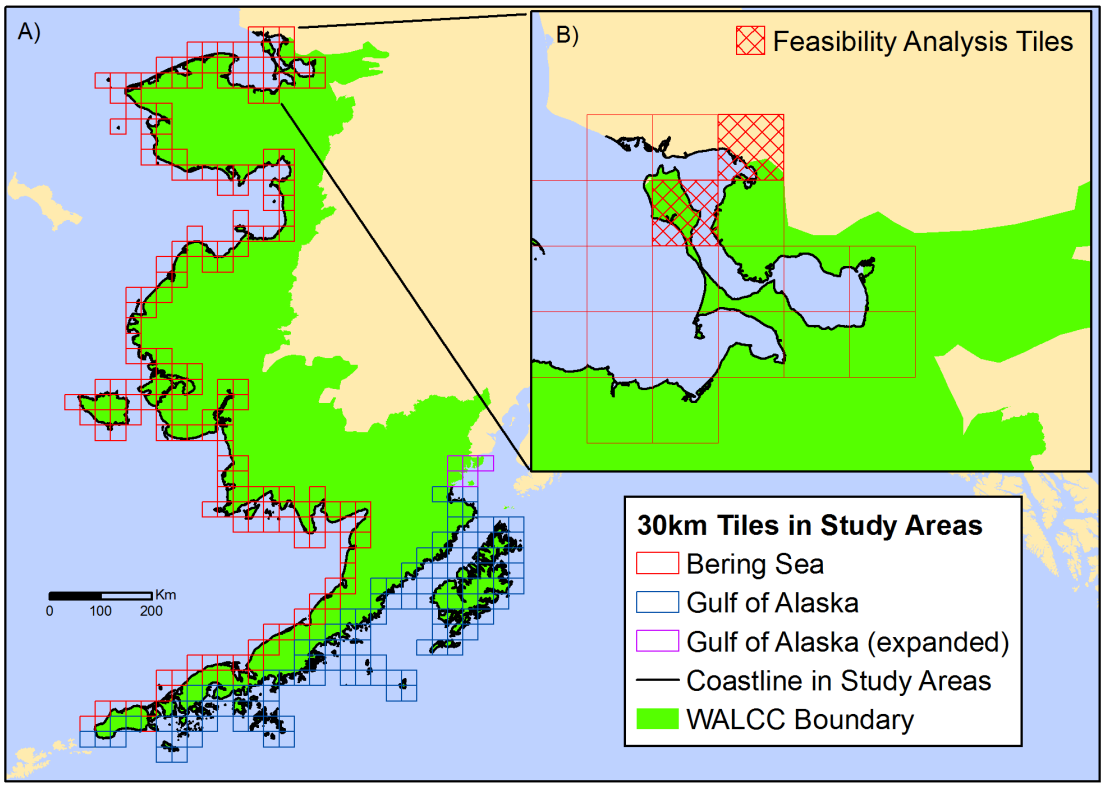

Figure 1. Study area and feasibility analysis tiles, Western Alaska LCC, Alaska.

The *Gulf of Alaska* study area includes the entire Gulf of Alaska coast within the bounds of the Western Alaska LCC (Figure 1, Map A). This area extends from Sennet Point to Chinitna Bay and includes Kodiak Island and associated archipelago, Chirikof Islands, Semidi Islands, Shumagin Islands, and Samak Island. Approximately 11,240 km of "coastline" are included within this study area, based on the Alaska 1:63,360 coastline map produced by the Alaska Department of Natural Resources in 1998. This total length includes outer and inner portions of barrier islands and various portions of river mouth channels. A total of 135 30-km Landsat tiles (defined under Methods: Preprocessing below) include portions of the Gulf of Alaska coast in the study area. Note that this is five more tiles than originally estimated because initially an earlier version of the WALCC boundary was used that ended at Kamishak Bay instead of Chinitna Bay. Since nine tiles include both the Bering Sea and Gulf of Alaska coast, a total of **327 tiles** cover all of the coast within the study area.

For the feasibility assessment, two tiles in Kotzebue Sound (near the northern boundary of the Western Alaska LCC) were selected (Figure 1, Map B) as the Landsat TM and ETM+ imagery was on hand from a previous project. The input data for these were carefully reviewed to exclude imagery with cloud contamination or other data quality problems over the coast.

METHODS

ASSESS AVAILABLE IMAGERY

SPATIAL COVERAGE THROUGH TIME

We analyzed the metadata for the extensive time series of Landsat imagery (1972–2012) covering Alaska and then reviewed the results for the Bering Sea coast and Gulf of Alaska coast within the boundary of the Western Alaska LCC. First, the complete metadata records for Landsat 1–7 were downloaded in comma-delimited text format (http://landsat.usgs.gov/metadatalist.php). Then, the shapefiles containing the "descending" (daytime) World Reference System 1 scene footprints (WRS1, used by Landsat 1–3) and World Reference System 2 scene footprints (WRS2, used by Landsat 4 and later) were downloaded (http://landsat.usgs.gov/tools_wrs-2_shapefile.php). The list of scene footprints intersecting Alaska was extracted for both WRS1 and WRS2. The metadata records that corresponded to

WRS1 or WRS2 footprints over Alaska were imported into a Microsoft Access 2010 database and SQL queries were developed to summarize the Landsat coverage that met date and cloud-cover criteria. One query counted the number of scenes for each path/row and each year that had 20% cloud cover or less and that were acquired during July, August, or September. A second query summed the cloud-free area by path/row and year for each scene acquired during June, July, August or September.

To map the coverage with the overlapping rows, the WRS1 and WRS2 footprint shapefiles were edited to eliminate the overlapping boundary between adjacent rows. Then the results of the SQL queries summarizing the coverage by path/row and year were joined to the footprint shapefile as additional columns. The coverage data for each year was then exported to a raster format at 1-km resolution. Because the Landsat paths overlapped, the set of paths was split into five groups for the raster export; then the five sets of rasters were summed together. The result was a raster that depicted the number of scenes that met the selected criteria for each sensor type (MSS or TM/ETM+) and year. The data were reviewed and multiple years of data were summed into summary rasters that depicted the overall extent of coverage within defined eras.

SENSOR COVERAGE

Landsat MSS scenes are the only imagery available from the first three Landsat satellites (primarily covering the time period 1972–1982). Landsat 4 and 5 collected both MSS and TM data (MSS only, TM only, or MSS and TM simultaneously). In general, the TM data are preferred. The MSS data are coarser resolution than TM and ETM+ data (~60-m pixels compared to 30-m pixels), and MSS data lack some of the spectral channels available with TM and ETM+. However, the MSS data are the best digital satellite imagery available for the earlier time periods. This is particularly important for some areas in western Alaska where little Landsat TM or ETM+ imagery is available prior to 1999.

CHANGE DETECTION DEMONSTRATION

IMAGE PREPROCESSING

Change detection methods were demonstrated for a set of tiles in the NE corner of the study region (Figure 1b) for which Landsat TM and ETM+ tile data (1985–2011) had already been

compiled as part of a National Park Service project assessing habitat conditions for the Western Arctic Caribou Herd. High quality scenes (mostly cloud-free and ice-free along the coast) were identified and ordered from the USGS, processed to top of atmosphere reflectance and surface reflectance (http://espa.cr.usgs.gov/). Landsat MSS browse imagery (1972–1992) was reviewed and high quality scenes were ordered from USGS via EarthExplorer.

Image preprocessing includes orthorectification, precision registration, radiometric calibration, atmospheric correction, and cloud masking. For Landsat MSS, TM and ETM+ imagery, the orthorectification and precision registration are already performed in the standard product. Landsat TM and ETM+ imagery was ordered in calibrated and atmospherically corrected format produced using the Landsat Ecosystem Disturbance Adaptive Processing System (LEDAPS) set of preprocessing routines (Masek 2006). The MSS data was converted to top of atmosphere reflectance using ENVI 5.0 software. Entirely or nearly cloud-free data were available across the two primary tiles of interest and so no cloud masking was required.

The imagery was reprojected and tiled into a statewide tiling scheme in the Alaska Albers (NAD 1983) coordinate system that ABR developed to facilitate the creation of time-series stacks from overlapping Landsat paths. The state is divided into non-overlapping square tiles 30 km to a side, or 1000 × 1000 30-m Landsat pixels. Two tiles of data (AKH062V16 and AKH063V15, Figure 1b) were produced using the Landsat MSS, TM, and ETM+ imagery.

CHANGE DETECTION: ANNUAL TIME SERIES

A goal of the analysis was to maximize the number of annual time steps, because this improves the robustness of the end result. Results from change detection analysis based on two time steps are highly dependent on conditions at the two dates selected, and are also affected by small co-registration errors between the two datasets. The higher number of observations (years) with the time-series stack approach provides greater sensitivity for the detection of long-term trends, when compared to a two-date change detection approach (Fraser 2011).

Natural intraannual variation in water levels and other coastline features that affect near-infrared reflectance can confound the analysis. Landsat data were selected to avoid sea ice; dates from mid- to late summer and early fall were preferred. In the northern portion of the study area used for the feasibility analysis, June and even early July imagery can have ice and snow drifts

along coastal bluffs. We intended to avoid imagery with snow or ice contamination; however, one early July 2001 scene with snow drifts along some coastal bluffs was included in the time series.

The focus of the change detection is on conversions between discrete cover types (e.g., tundra, barrens, water), rather than on subtle transitions within and among vegetation types. Thus, constraints on timing to ensure consistent phenology were relaxed, increasing the number of time steps available and reducing the effort required for manual cloud masking. However, this approach also means that the results are less useful for assessing vegetation community and structure changes in consistently vegetated portions of the study area.

SPECTRAL METRICS

For the feasibility analysis, we focused on a single spectral metric: near-infrared reflectance (NIR). The MSS data have two near-infared bands; we selected the second of these bands (~0.8–1.1 μm) because it was less noisy and less affected by atmospheric variations. Other potential metrics include Normalized Difference Vegetation Index (NDVI; Rouse 1976, Macander 2011 and Fraser 2011), short-wave infrared reflectance (SWIR) (Landsat TM or ETM+ bands 7; Macander 2011), and Tasseled Cap Wetness (Wetness; Crist 1984, Kennedy 2010 and Macander 2011). However, NDVI is optimized to detect changes in vegetation vigor or abundance rather than changes between non-vegetated states (e.g. water to barrens). Also, by definition, it includes more than one MSS band (red and near-infrared) and the red band was frequently noisy. The SWIR and Wetness metrics are not available with MSS data since it lacks a detector in the SWIR wavelengths.

The change detection was performed over the entire four decade time series (1972-2011). A linear regression was performed for each pixel, with year as the explanatory variable. The slope of the regression line yielded the annual rate of change in the selected metric. The statistical significance of the change for each pixel was also assessed. The resulting maps are filtered to depict areas with significant change ($p < 0.05$). The magnitude and direction of spectral change was produced as a raster layer.

A classification model was developed to categorize spectral change into land cover transitions. For the feasibility assessment a simple “water to land” and “land to water” transition

model was developed based on the clear distinction between these classes in the near-infrared. Other spectral changes that were not as easy to interpret were flagged as increasing or decreasing NIR.

Temporal and Sensor Subsets

In addition to the full time series, several temporal subsets of tile AKH063V916 were analyzed (Table 1). To interpret the images used for each subset, review the column below the title of the "feasibility analyses"; for example, the "full time series" included all the scenes except for the 1986 MSS scene (this was excluded because the TM scene from the same date was used instead). The analysis of the temporal subsets allowed us to assess the ability of the method to perform using only MSS data; to distinguish decadal scale patterns; and to assess the performance when only 1970s and 2000s imagery are available. The latter test was performed because for some portions of the study area little or no suitable imagery was acquired during the 1980s and 1990s.

RESULTS AND DISCUSSION

ASSESS AVAILABLE IMAGERY

The available imagery was summarized using two different approaches. First, the count of scenes acquired in July, August and September with estimated cloud cover of 20% or less was calculated and mapped (Figure 2). These are generally very high quality scenes with extensive cloud-free coverage. However, scenes of this quality are rare, particularly for areas with persistent cloud cover such as the Alaska Peninsula. When the coverage was summarized for different sensors and eras, a clear pattern emerged with extensive data available north of the Yukon-Kuskokwim Delta, sparser coverage for Bristol Bay and the Alaska Peninsula, and moderate coverage for Kodiak Island and adjacent mainland. Temporally, coverage from the MSS sensor was high during the 1970s and TM/ETM+ coverage was high following the launch of Landsat 7 in 1999. Coverage during the 1980s and 1990s was patchy, with large expanses of the YK Delta and Alaska Peninsula having coverage from 2 or fewer scenes during particular eras.

The second method of summarizing available imagery used a weighted approach instead of a cloud cover threshold. The cloud-free portion of each scene in the archive was calculated and the total coverage of cloud-free area was summed (Figure 3). In addition, the first summary demonstrated that the northern portion of the study area had very good coverage. In the north, sea ice is more prevalent and melt occurs later. Therefore the seasonal threshold was July through September. For the second analysis of available imagery we extended the seasonal threshold to include June scenes as well since snow and ice are less likely to persist on the coast into June in the southern portion of the study area.

The weighted approach is a better indicator of overall data availability. In areas with persistent cloud cover such as the Alaska Peninsula it is frequently necessary to take advantage of cloud-free portions of imagery rather than relying on scenes that are mostly or entirely cloud-free. Based on the weighted cloud-free coverage approach (Figure 3), robust imagery coverage with six or more scenes per era is available across the entire study area during two eras of the 1970s (1972–1975 and 1976–1979) and 2000s (1999–2005 and 2006–2012). There are areas with sparser data for the 1980s and 1990s, particularly for the period 1987–1998.

CHANGE DETECTION

ANNUAL TIME SERIES

An annual time series was constructed for the two primary tiles of the feasibility analysis. The annual time series for tile AKH062V16 is listed in Table 1 and depicted using three bands to produce a color infrared images in Figure 4. Striping is visible in many of the MSS scenes, particularly 1972 and 1979; however, the second near-infrared band did not have major striping visible in any of the scenes used for the analysis. Gaps are visible in the ETM+ scenes from 2003 and later and are seen as solid black. The gap areas were treated as no data during the statistical analysis. Seasonal differences are evident; for example, the 1981, 1984, 1987, 2005 and 2011 data were acquired in September and the bright red shrubby areas clearly visible in most other years have senesced. The earliest acquisition date was July 8 in 2001; substantial snow drifts are still visible along the west coast and at several inland locations. The snow could confound the analysis especially if it occurred above seasonal ice along the shore (i.e. over areas that would be open water after melt). The snow surface is bright in the near-infrared and would be interpreted as land. For the final analysis the input imagery will be visually screened to exclude scenes with coastal snow and ice.

Table 1. Landsat scenes used for each of the time series feasibility analyses, tile AKH063V16. ‘X’ denotes image was used in the analysis.

				Feasibility Analyses							
Acquisition Date	Satellite	Sensor	WRS/Path/Row	Full Time Series	Full Time Series with 20-year Gap	MSS 1972–1983	MSS 1983–1992	MSS 1972–1992	TM 1986–2001	TM 2001–2011	TM 1986–2011
1972-07-31	Landsat 1	MSS	WRS1/P72/R13	X	X	X		X			
1974-08-06	Landsat 1	MSS	WRS1/P74/R13	X	X	X		X			
1975-07-24	Landsat 2	MSS	WRS1/P75/R13	X	X	X		X			
1977-07-12	Landsat 2	MSS	WRS1/P77/R13	X	X	X		X			
1978-07-16	Landsat 3	MSS	WRS1/P78/R13	X	X	X		X			
1979-07-12	Landsat 3	MSS	WRS1/P79/R13	X	X	X		X			
1980-08-21	Landsat 2	MSS	WRS1/P80/R13	X		X		X			
1981-09-19	Landsat 2	MSS	WRS1/P81/R13	X		X		X			
1983-07-23	Landsat 4	MSS	WRS2/P83/R13	X		X	X	X			
1984-09-03	Landsat 5	MSS	WRS2/P84/R13	X			X	X			
1985-07-20	Landsat 5	MSS	WRS2/P85/R13	X			X	X			
1986-08-24	Landsat 5	TM	WRS2/P86/R13	X					X		X
1986-08-24	Landsat 5	MSS	WRS2/P86/R13				X	X			
1987-09-19	Landsat 5	TM	WRS2/P87/R13	X					X		X
1990-08-10	Landsat 5	TM	WRS2/P90/R13	X					X		X
1992-07-31	Landsat 4	MSS	WRS2/P92/R13	X			X	X			
1999-07-28	Landsat 7	ETM+	WRS2/P99/R13	X	X				X		X
2000-07-21	Landsat 7	ETM+	WRS2/P00/R13	X	X				X		X
2001-07-08	Landsat 7	ETM+	WRS2/P01/R13	X	X				X	X	X
2002-07-27	Landsat 7	ETM+	WRS2/P02/R13	X	X					X	X
2003-08-24	Landsat 7	ETM+	WRS2/P03/R13	X	X					X	X
2004-08-26	Landsat 7	ETM+	WRS2/P04/R13	X	X					X	X
2005-09-05	Landsat 7	ETM+	WRS2/P05/R13	X	X					X	X
2006-08-31	Landsat 5	TM	WRS2/P06/R13	X	X					X	X
2008-08-20	Landsat 5	TM	WRS2/P08/R13	X	X					X	X
2009-08-16	Landsat 5	TM	WRS2/P09/R13	X	X					X	X
2010-07-09	Landsat 5	TM	WRS2/P10/R13	X	X					X	X
2011-09-06	Landsat 7	ETM+	WRS2/P11/R13	X	X					X	X

Figure 2. Count of Scenes with Cloud Cover <= 20%, July–September

Fig02_Feasibility_Results_CC20_789_13-321.mxd 5/17/2013

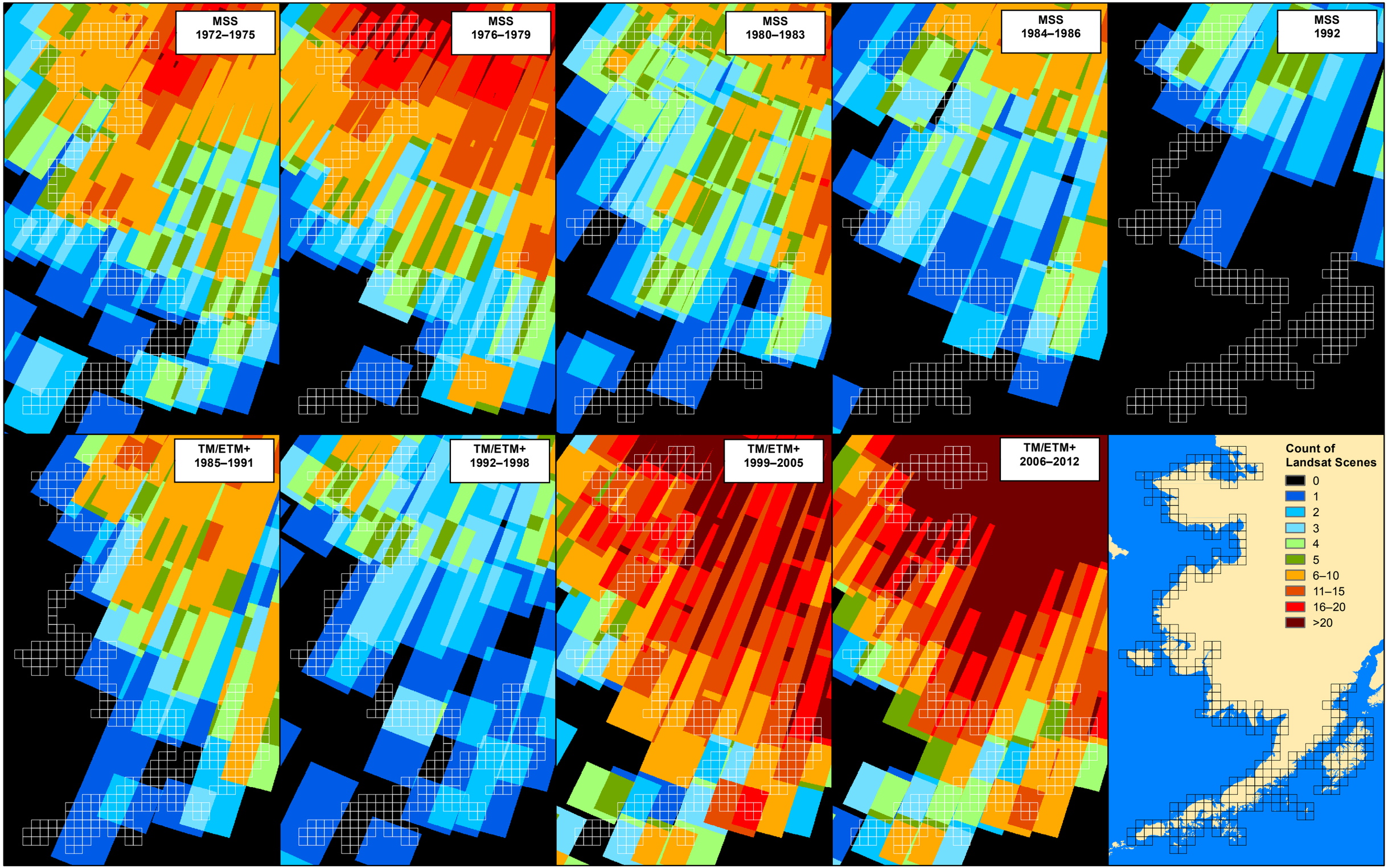

Figure 3: Weighted Count of Cloud-Free Coverage, June–September.

Fig03_Feasibility_Results_Weighted_6789_13-321.mxd 5/17/2013

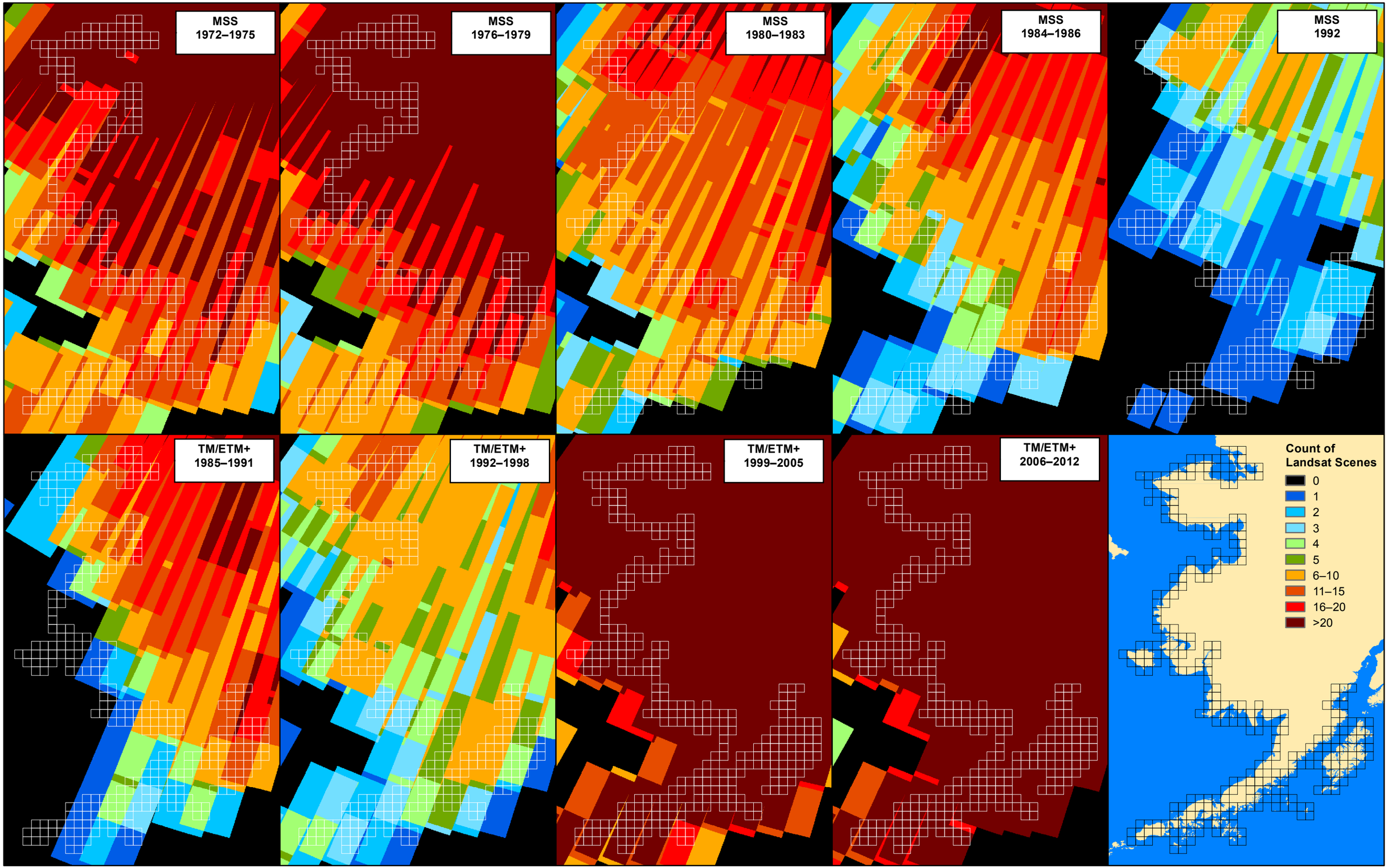

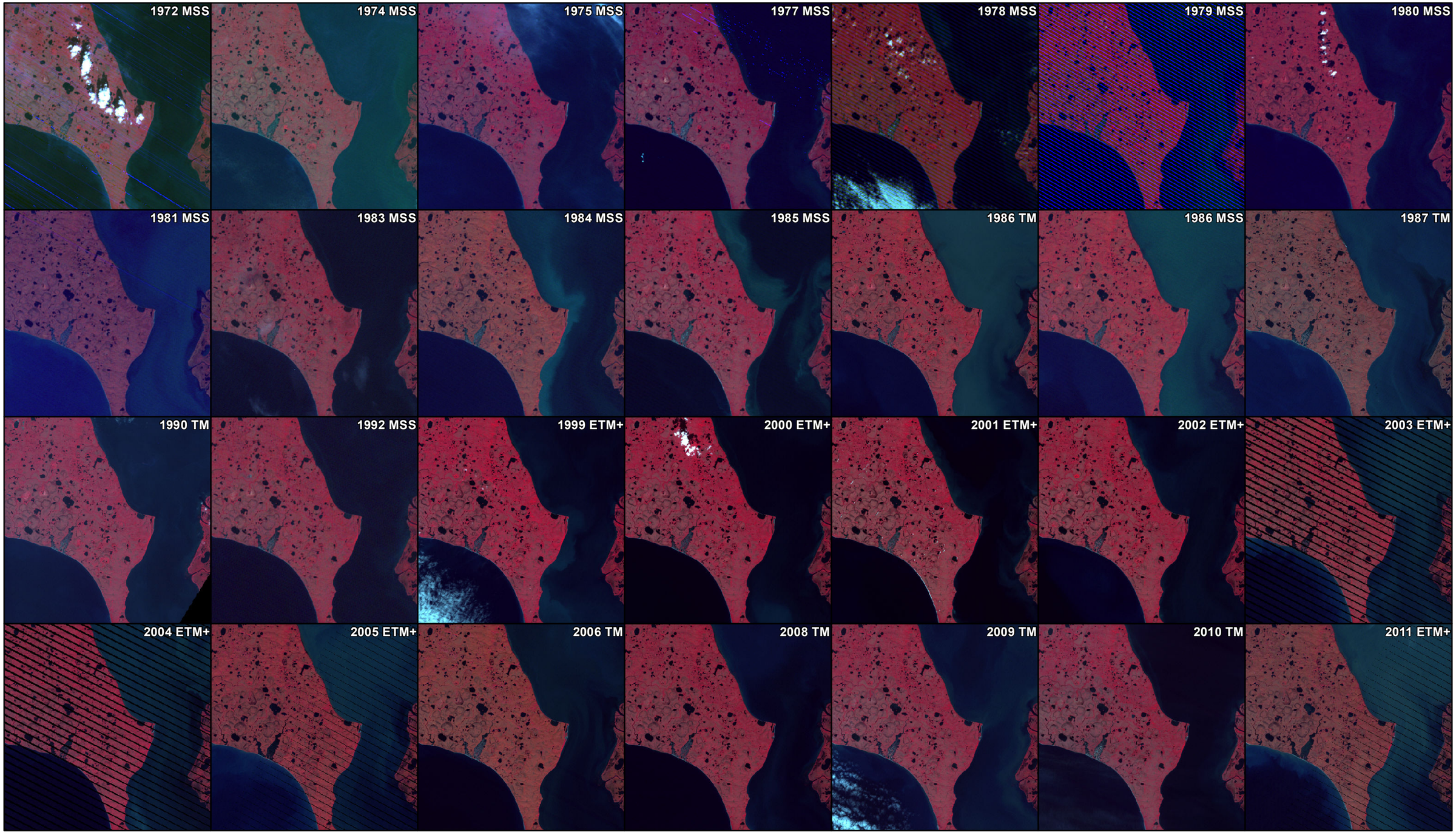

Figure 4. Landsat Time Series for tile AKH063V16.

Fig04_Landsat_Time_Series_AKH062V16_13-321.mxd 5/17/2013

AKH062V16: Landsat Trend Analysis Results,
Full Time Series (1972–2011, 28 years with data)
All Significant Spectral Change
Displayed over 2010 Imagery

- 1=Land to Water
- 2=Water to Land
- 3=Other Change (Decreasing NIR)
- 4=Other Change (Increasing NIR)
- 5=No Significant NIR Change

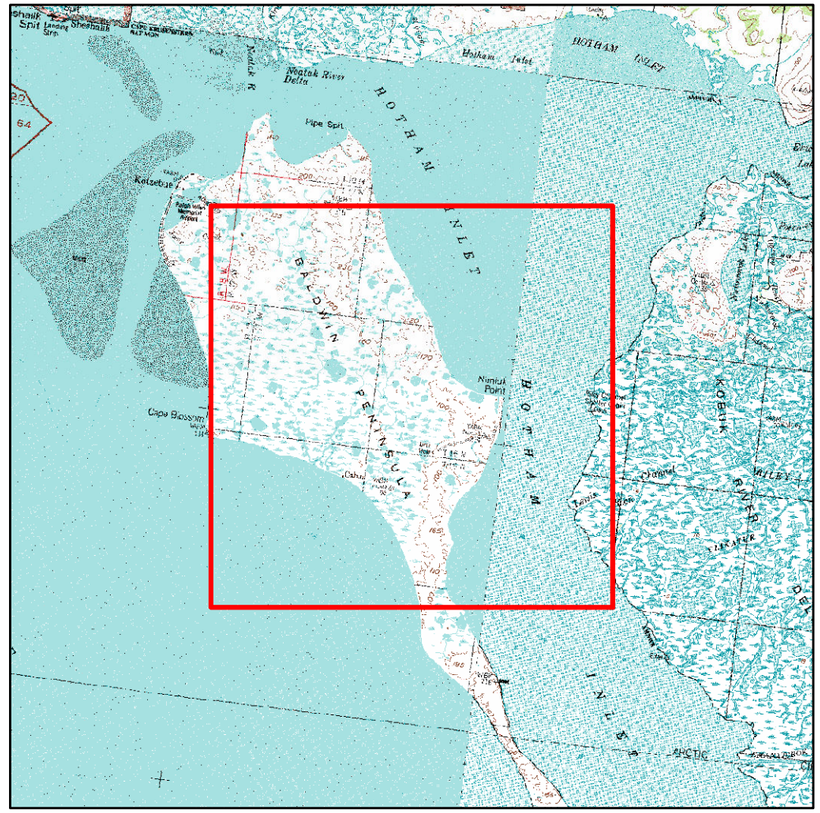

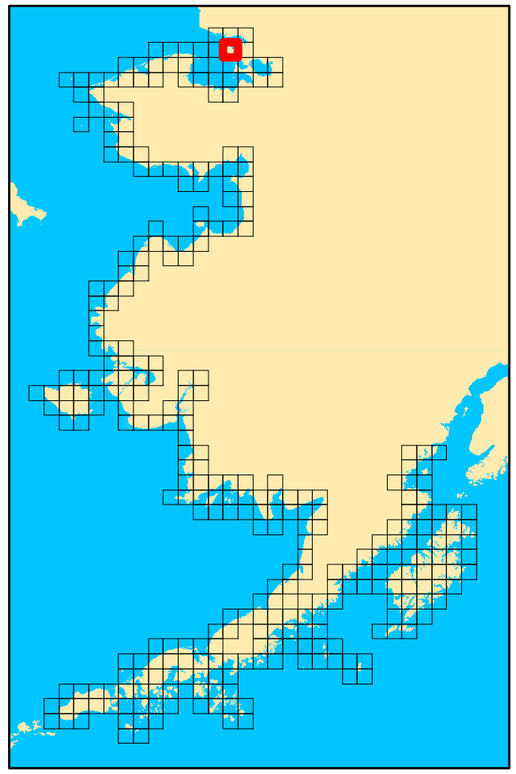

0 1 2 3 Km

Figure 5. Landsat trend analysis results for full time series 1972–2011, tile AKH062V16. All significant near-infrared spectral change.

Fig05_Results_Full_Time_Series_AKH062V16_All_Sig_Change_13-321.mxd 5/17/2013

SPECTRAL METRICS

For the feasibility analysis, the selected spectral metric was near-infrared reflectance (NIR). For MSS, which has two NIR bands, the second band was used (~0.8–1.1 μm). This is referred to as Band 7 on Landsat 1–3 and Band 4 on Landsat 4–5. For Landsat TM and ETM+, the single infrared band (Band 4) was used. Open water is very dark in the near-infrared while barrens and green vegetated land surface, and senesced vegetated land surfaces are all much brighter. Near-infrared reflectance is available in both MSS and TM/ETM+ imagery and is fairly insensitive to atmospheric effects as well as water turbidity.

The results of the spectral change detection for tile AKH062V16 show widespread change, dominated by increased NIR over land (Figure 5). For this and other figures depicting the spectral change results, areas with no trend are not colored, and show the underlying color-infrared imagery. Only areas with significant spectral change ($p < 0.05$) are shown. Most of the detected spectral change is not relevant to coastal processes. The change over land may be related to increased shrub cover but could also be a spurious result due to the loose seasonal constraints on the time series, or the somewhat different bandpasses for near-infrared reflectance across MSS, TM and ETM+ sensors. The change detection approach used for this study is not expected to reliably capture subtle changes in vegetation cover or structure over time.

To focus on conversions relevant to coastal changes, a simple model was developed to capture transitions from land (high NIR) to water (low NIR) and vice versa. Based on examination of image histograms (see Figure 6 for an example) there was a clear bimodal distribution with water having a narrow distribution with a peak at low values and land surfaces having a broader distribution with a peak at higher values (reflectance is scaled by 10,000 in the calibrated imagery and in Figure 6). A threshold of 750 (corresponding to a reflectance of 0.075) was identified that separated the water and land.

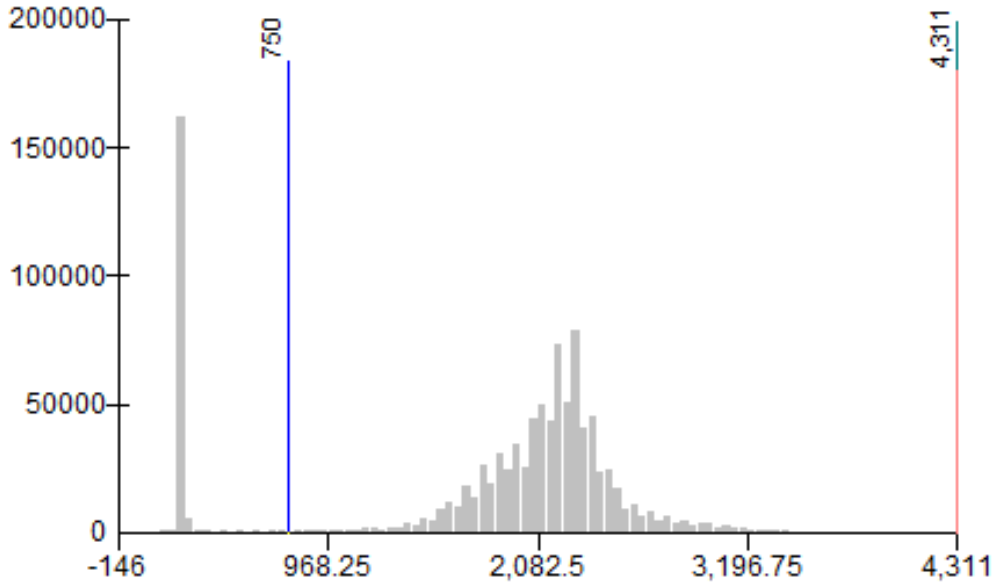

Figure 6. Histogram of near-infrared reflectance for tile AKH063V15, 1975.

The trend analysis results were used to estimate near-infrared reflectance at the start and end of the time series by taking the mean value and adding (or subtracting) the rate of change times half the number of years in the time series. This provided a "clean" NIR at the start and end of the time series with the interannual variation stripped out. For pixels without significant change, the NIR reflectance was the same at the start and end of the time series.

Then, pixels that changed from less than 750 to more than 750 were categorized as "water to land". Pixels that changed from more than 750 to less than 750 were categorized as "land to water". The rest of the changes were then classified as "increasing NIR" or "decreasing NIR" based on the sign of the slope coefficient.

By focusing on land to water and water to land conversions, a map of changes focused on those that were relevant to coastal change processes was produced (Figure 7). The depth of the time series (28 years during the 1972–2011 time period) and the statistical significance threshold provide confidence that the changes detected are real and persistent, rather than being driven by anomalously high or low water levels or other temporary conditions in a small number of unusual years. Although the method should be fairly resistant to bias from such extremes, it would be best to avoid imagery acquired during extreme conditions. If historical, time-stamped

AKH062V16: Landsat Trend Analysis Results,
Full Time Series (1972–2011, 28 years with data)
Major Land Cover Conversions
Displayed over 2010 Imagery

1=Land to Water

2=Water to Land

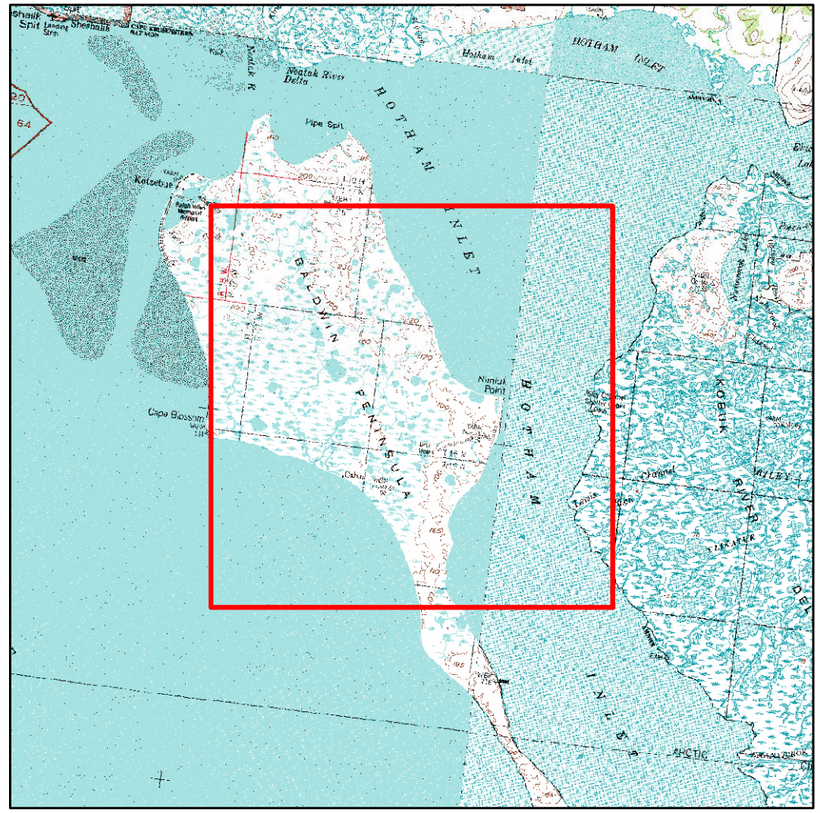

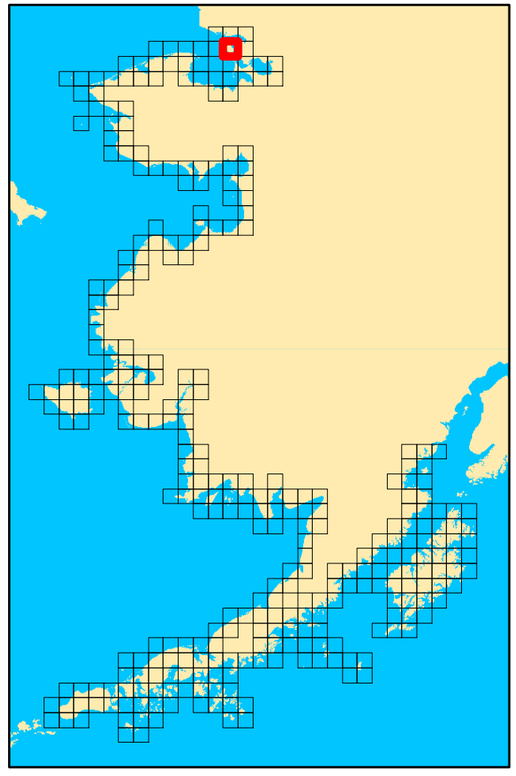

Km
0 1 2 3

Figure 7. Landsat trend analysis results for full time series 1972–2011, tile AKH062V16. Significant near-infrared spectral change classified as land to water or water to land conversion.

Fig07_Results_Full_Time_Series_AKH062V16_Conversions_13-321.mxd 5/31/2013

Figure 8. Landsat trend analysis results for full time series 1974–2011, tile AKH063V15. All significant near-infrared spectral change.

AKH063V15: Landsat Trend Analysis Results, Full Time Series (1974–2011, 26 years with data)
All Significant Spectral Change
Displayed over 2010 Imagery

- 1=Land to Water
- 2=Water to Land
- 3=Other Change (Decreasing NIR)
- 4=Other Change (Increasing NIR)
- 5=No Significant NIR Change

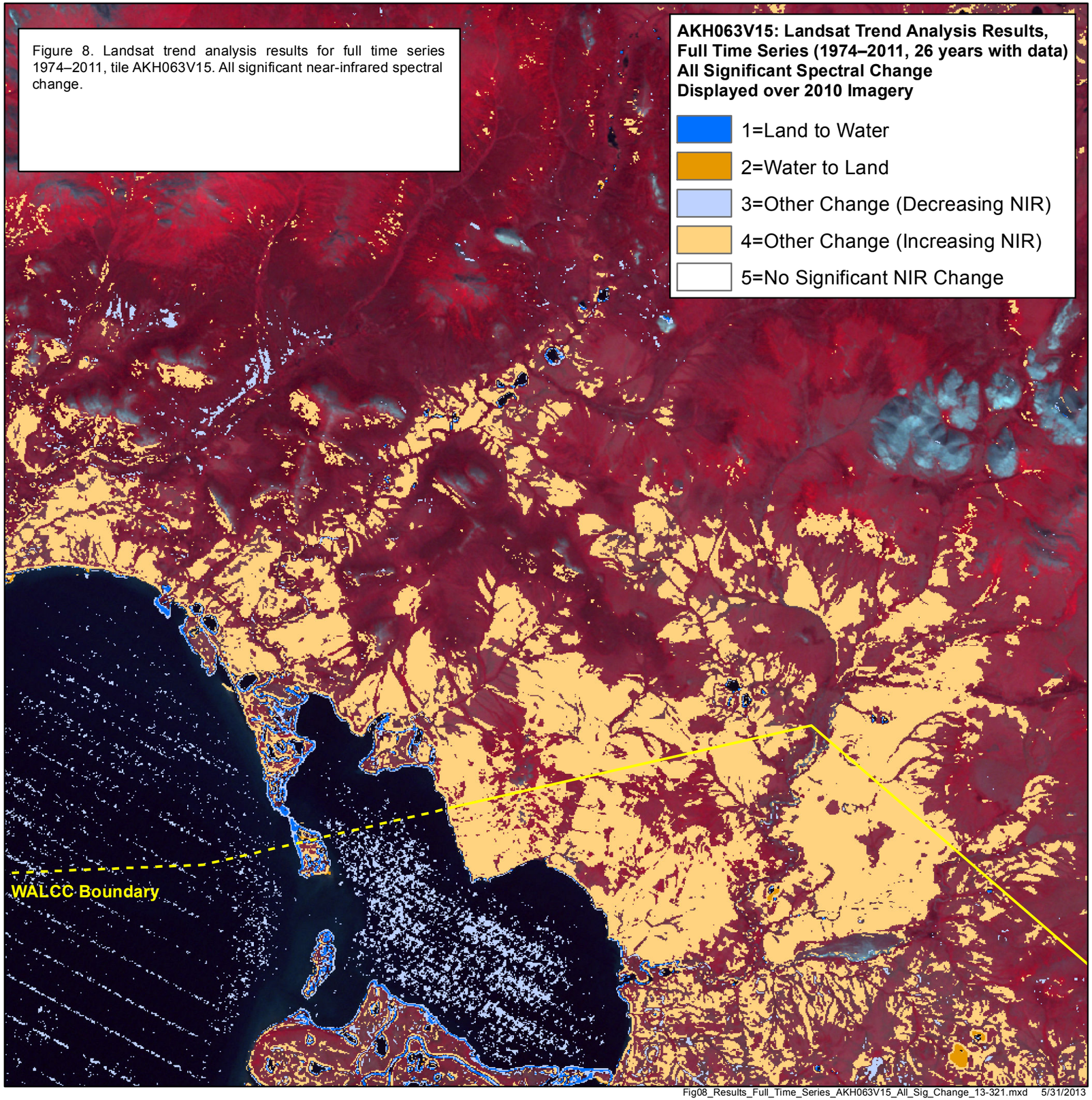

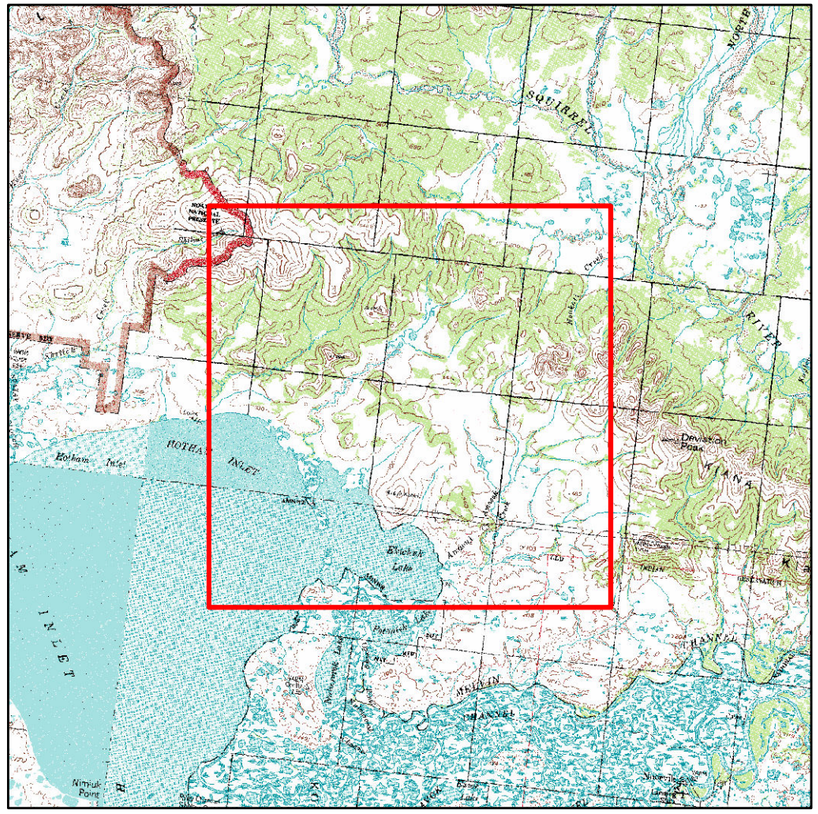

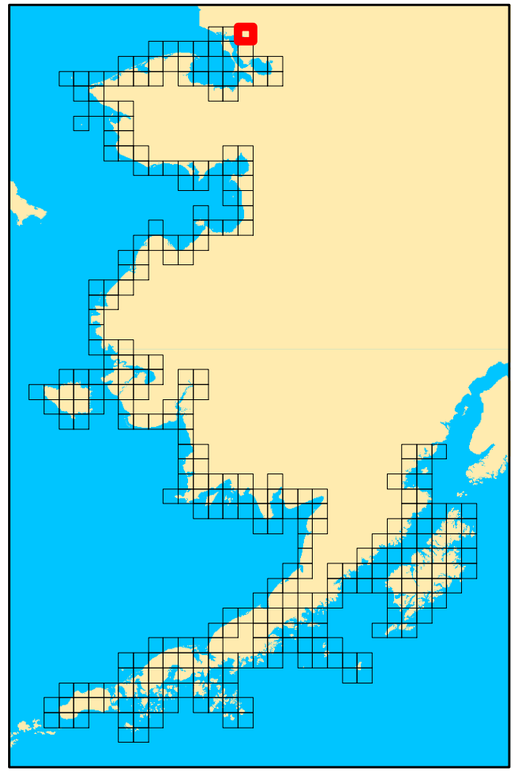

0 1 2 3 Km

Fig08_Results_Full_Time_Series_AKH063V15_All_Sig_Change_13-321.mxd 5/31/2013

Figure 9. Landsat trend analysis results for full time series 1974–2011, tile AKH063V15. Significant near-infrared spectral change classified as land to water or water to land conversion.

AKH063V15: Landsat Trend Analysis Results, Full Time Series (1974–2011, 26 years with data) Major Land Cover Conversions Displayed over 2010 Imagery

1=Land to Water

2=Water to Land

WALCC Boundary

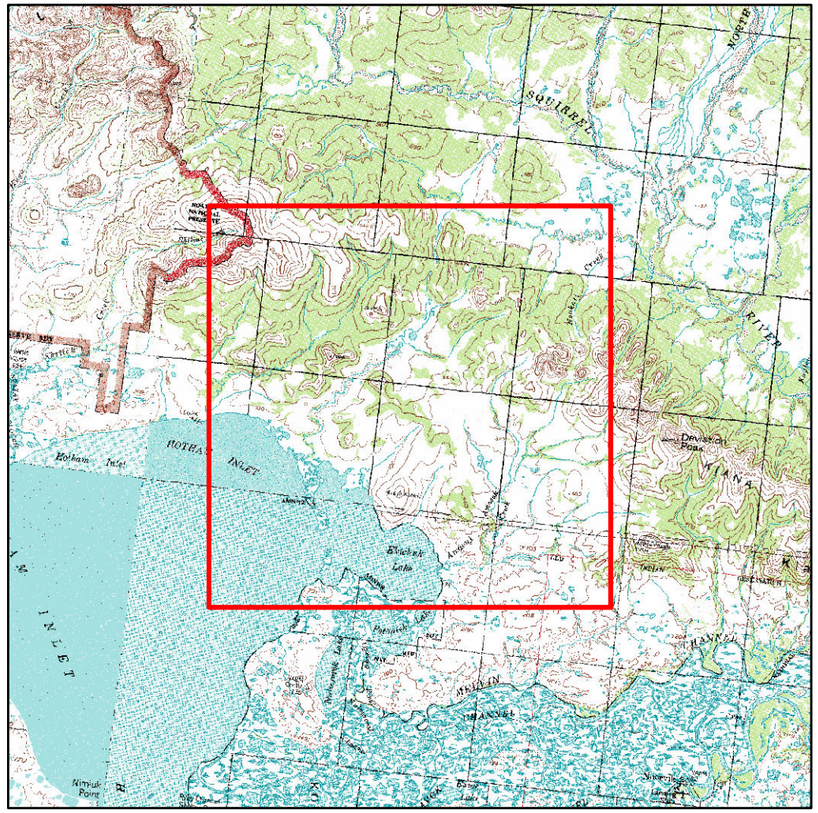

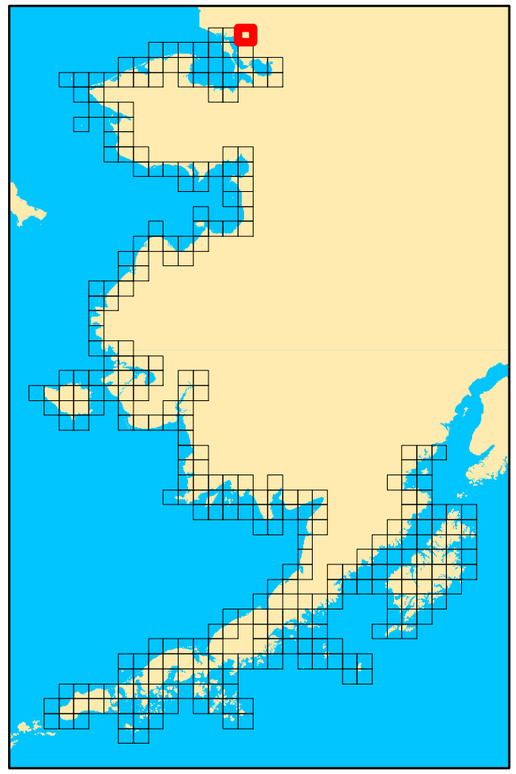

0 1 2 3 Km

Fig09_Results_Full_Time_Series_AKH063V15_Conversions_13-321.mxd 5/31/2013

AKH062V16: Landsat Trend Analysis Results, MSS 1972–1983 (9 years with data)
Major Land Cover Conversions
Displayed over 1983 Imagery

1=Land to Water

2=Water to Land

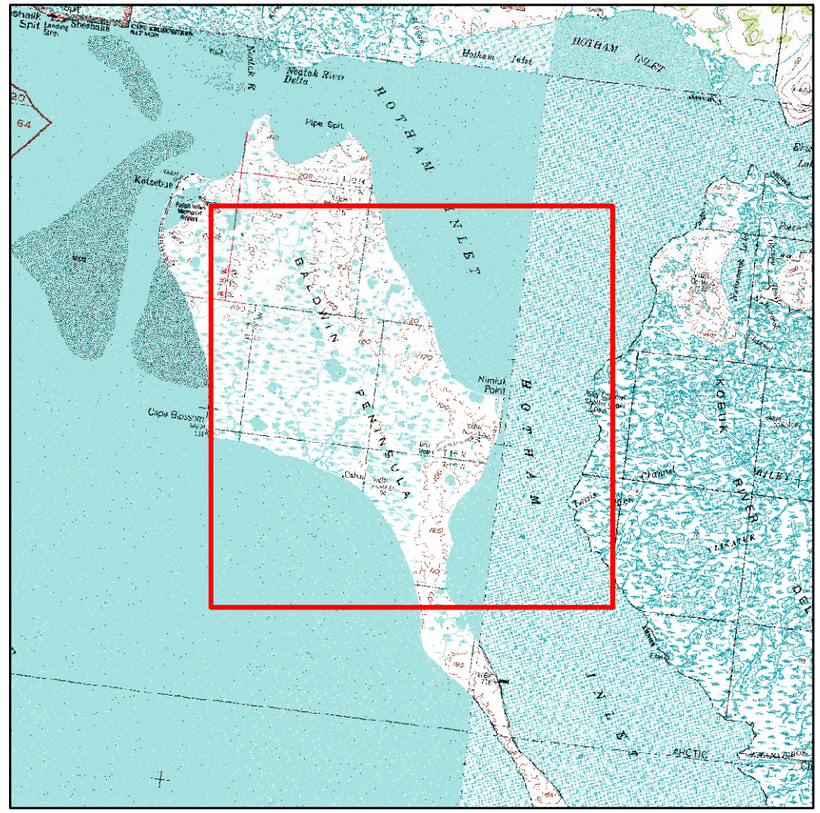

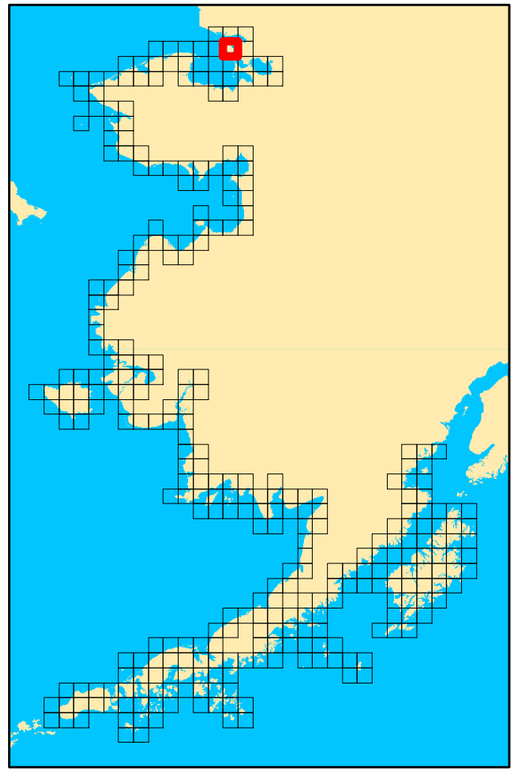

0 1 2 3 Km

Figure 10. Landsat trend analysis results for MSS 1972–1983, tile AKH062V16. Significant near-infrared spectral change classified as land to water or water to land conversion.

Fig10_Results_MSS_1972_1983_AKH062V16_Conversions_13-321.mxd 5/31/2013

AKH062V16: Landsat Trend Analysis Results, MSS 1983–1992 (5 years with data)
Major Land Cover Conversions
Displayed over 1992 Imagery

1=Land to Water

2=Water to Land

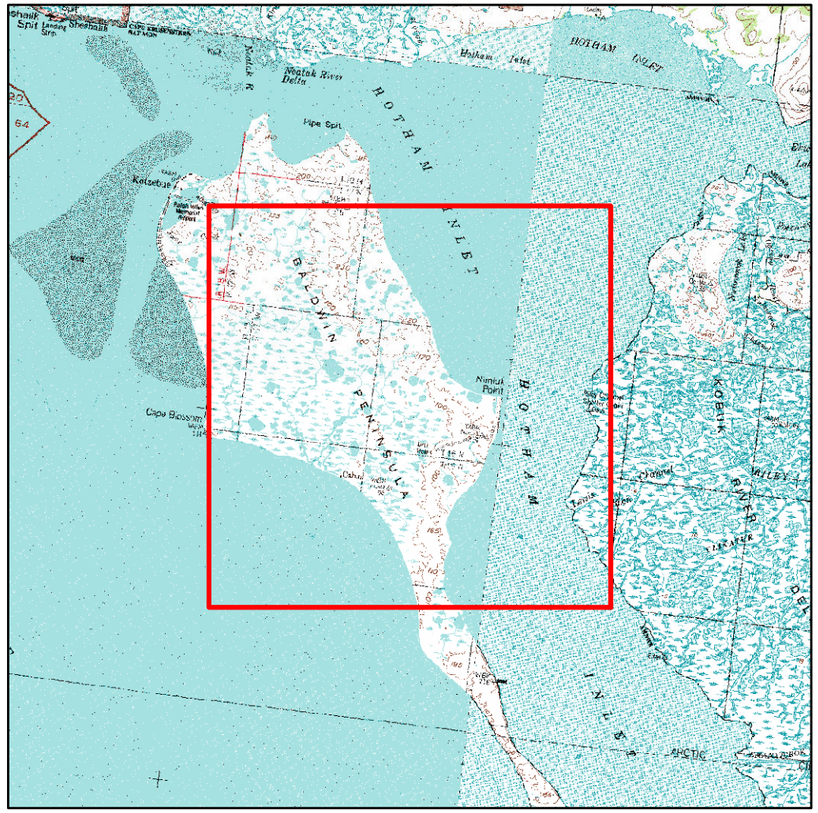

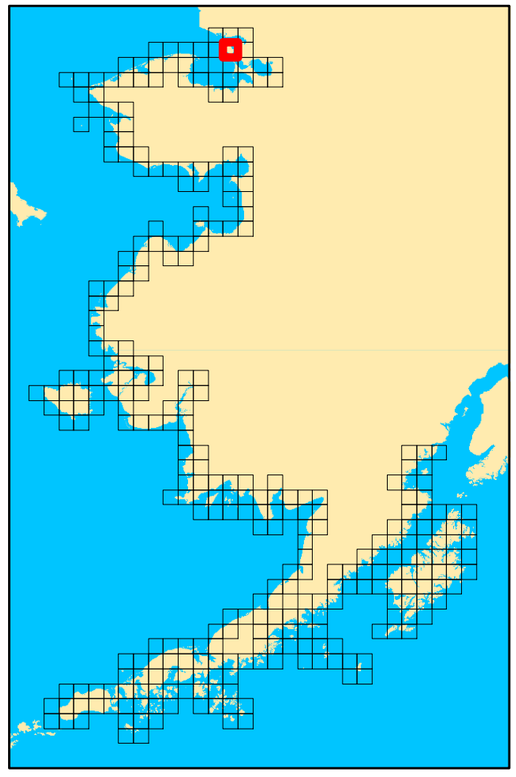

0 1 2 3 Km

Figure 11. Landsat trend analysis results for MSS 1983–1992, tile AKH062V16. Significant near-infrared spectral change classified as land to water or water to land conversion.

Fig11_Results_MSS_1983_1992_AKH062V16_Conversions_13-321.mxd 5/31/2013

AKH062V16: Landsat Trend Analysis Results, MSS 1972–1992 (13 years with data)
Major Land Cover Conversions
Displayed over 1992 Imagery

1=Land to Water

2=Water to Land

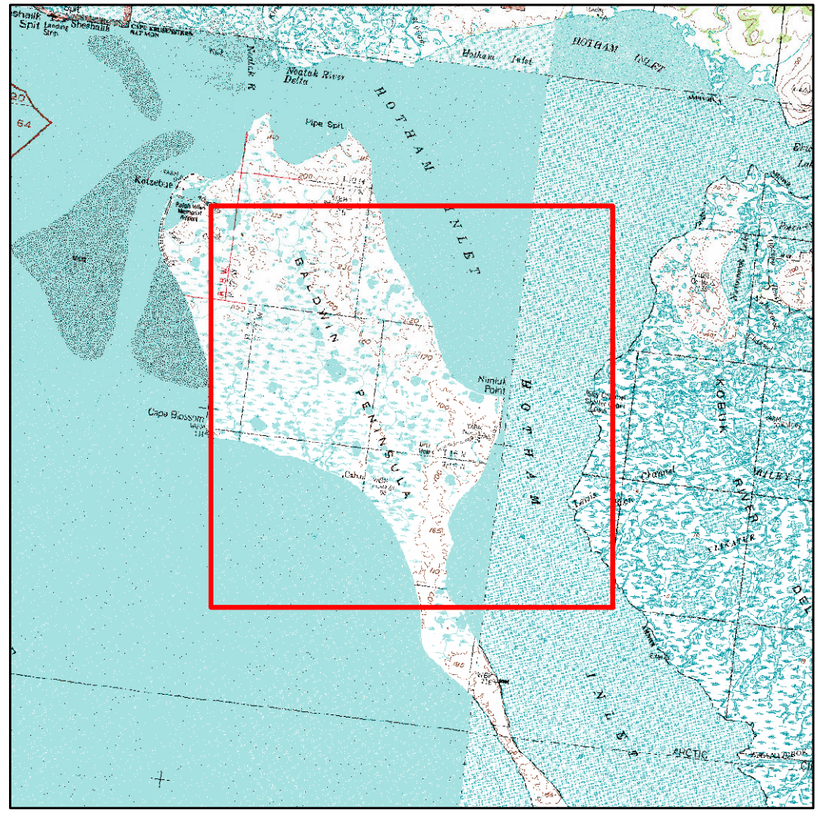

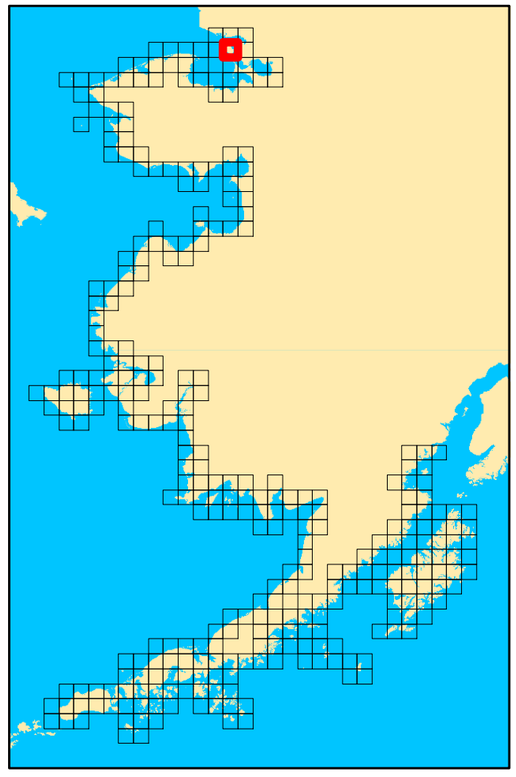

0 1 2 3 Km

Figure 12. Landsat trend analysis results for MSS 1972–1992, tile AKH062V16. Significant near-infrared spectral change classified as land to water or water to land conversion.

Fig12_Results_MSS_1972_1992_AKH062V16_Conversions_13-321.mxd 5/31/2013

water-level information relating to tides and/or storm surges is available it should be possible to link this information to the satellite imagery, which has very accurate time and date information. This could improve the results by screening out imagery with extreme, ephemeral conditions.

There are linear areas along several portions of the coast with land to water conversions, indicating coastal erosion. There is a water to land conversion adjacent to a lagoon near the center of the tile which could indicate migration of the barrier feature, though the conversion feature here is narrow enough (mostly one 30-m pixel) that it could be an artifact of the change in resolution between MSS (60-m pixels) and TM/ETM+ (30-m pixels). For the final analysis when combining MSS and TM/ETM+ imagery, aggregate the input data to 60-m rather than super-sampling the MSS data to 30-m will be evaluated. Such an aggregation approach should filter out detected changes that are due to the difference in resolution.

There is a major block of land to water conversion detected near the point at the center of the tile (Figure 7). A lagoon was constructed here by humans, with construction appearing to begin sometime between 1992 and 1999 (Figure 4). There are also extensive areas of land to water conversion along estuaries as well as along many interior lakes, though some of the one-pixel wide changes along lakes may be due to the resolution difference discussed above. Finally, the method clearly identifies several lakes that have partially or completely drained during the 1972–2011 time period.

A similar analysis with a slightly different set of input imagery was performed for tile AKH063V15 (Figure 8), located northeast of tile AKH062V16. Note that tile AKH063V15 is located on the border of the WALCC and several of the more pronounced changes in this tile occur in the adjacent Northwest Boreal LCC. There are extensive significant spectral changes with widespread increasing NIR on land and decreasing NIR along the coast and in open water. Much of the increasing NIR is associated with recovery on 1970s firescars; the burned areas can be seen clearly in the 1970s MSS imagery. NIR increases also occur on other, mostly shrubby slopes. Classified to land cover conversions (Figure 9), there is a much cleaner map with substantial erosion along some exposed coastal features, expansion of flooded areas on islands, and further inland, three drained lakes. An animation of the tile time series shows the gradual coastline changes occurring over the 1974–2011 time period which are captured by the land

cover conversion classification. The animation runs through the time-series quickly, covering the 1974–2011 time period in about 5 seconds. Then the animation displays the "clean" land cover conversions for 1 second, followed by the complete map of spectral change for 1 second. Setting the viewing application to auto-repeat is useful since a feature of interest can then be watched repeatedly; we found that watching the same feature over time multiple times in rapid succession was more productive than watching it once at a slow speed. The viewing speed can be adjusted within the viewing application (such as Windows Media Player). An optimal default playback speed can be determined for the final product.

Temporal and Sensor Subsets

The NIR spectral change and land cover conversion classification was run for several subsets of the time series for tile AKH062V16. This provides examples of the capabilities of MSS vs. TM/ETM+ imagery as well as the ability to map changes occurring over shorter time scales. Figures 10 and 11 show results for two decade long periods with MSS imagery (1972–1983 and 1983–1992, respectively). Only minor coastline changes are detected during each of these two decades with more conversions occurring in the delta along the southwest coast and inland lake drainage. The change detection over the full time series of MSS imagery (Figure 12, 1972–1992) identified some larger coastline changes with erosion on the southwest coast and accretion along the northeast coast of the Baldwin Peninsula. In addition lake drainage was captured, with somewhat larger drained areas identified than with the combination of the two decades individually. For this sample tile, the longer two-decade MSS time record appears to perform better than the shorter decadal time records. This is likely because the greater sample size reduces the impact of noise in the MSS data and also dampens the influence of interrannual variability.

Figures 13 and 14 depict results from two short TM/ETM+ eras (1986–2001 and 2001–2011, respectively). Extensive patches of land to water conversion are identified off the northeast coast of the Baldwin Peninsula in the 1986–2001 time series. However, these do not show up in the full 39-year time series (Figure 7). Review of the time series suggests that this "conversion" may be an artifact related to a low tide (revealing organic materials and causing foam from wave action) in the early 1986 and 1987 time steps of the 1986–2001 time series. Two development phases of the manmade lagoon at Nimiuk Point are identified in Figures 13 and 14. The full

TM/ETM+ time series (1986–2011, Figure 15) captures the total change in the manmade lagoon along with some erosion along the northeast and southwest coast of the Baldwin Peninsula.

Analysis of the tile including the Kobuk River Delta identified several low-lying areas as converting to water in the full TM/ETM+ tile series. The changes identified on the Delta over the 1986–2011 time period are more extensive than the changes identified for the two shorter periods (1986–2001 or 2001–2011) and also more extensive than the changes identified for the full 39-year time series. The 39-year time series did show significant spectral change (decreasing NIR) in these areas but the estimated NIR at the end point did not meet the threshold to be classified as a land to water conversion. This suggests that the threshold or other details of the classification algorithm should be reviewed and refined further for the full analysis. We do anticipate a major algorithm refinement effort as part of the full analysis.

A final temporal subset excluded data from 1980–1999; this time series included Landsat MSS data from 1972–1979 and Landsat TM/ETM+ data from 1999–2012. The assessment of available imagery indicated that for some of the study area (primarily portions of the Yukon-Kuskokwim Delta and the Alaska Peninsula), minimal Landsat imagery was acquired during the 1980s and 1990s. The results of the time series analysis for tile AKH062V16 with 1980–1998 data withheld (Figure 16) show how the approach would work with a 20-year gap. Overall the results are very similar to the full 39-year time series (Figure 7). There are minor differences but the major coastal erosion features and lake drainage features are nearly the same. The consistent results between analyses using the full 39-year time series and the 39-year time series with a 20-year gap provide good evidence that the change detection technique can be applied to portions of the study area with good data at the start and end of the time period, but substantial gaps during the middle.

AKH062V16: Landsat Trend Analysis Results, TM 1986–2001 (6 years with data)
Major Land Cover Conversions
Displayed over 2001 Imagery

1=Land to Water

2=Water to Land

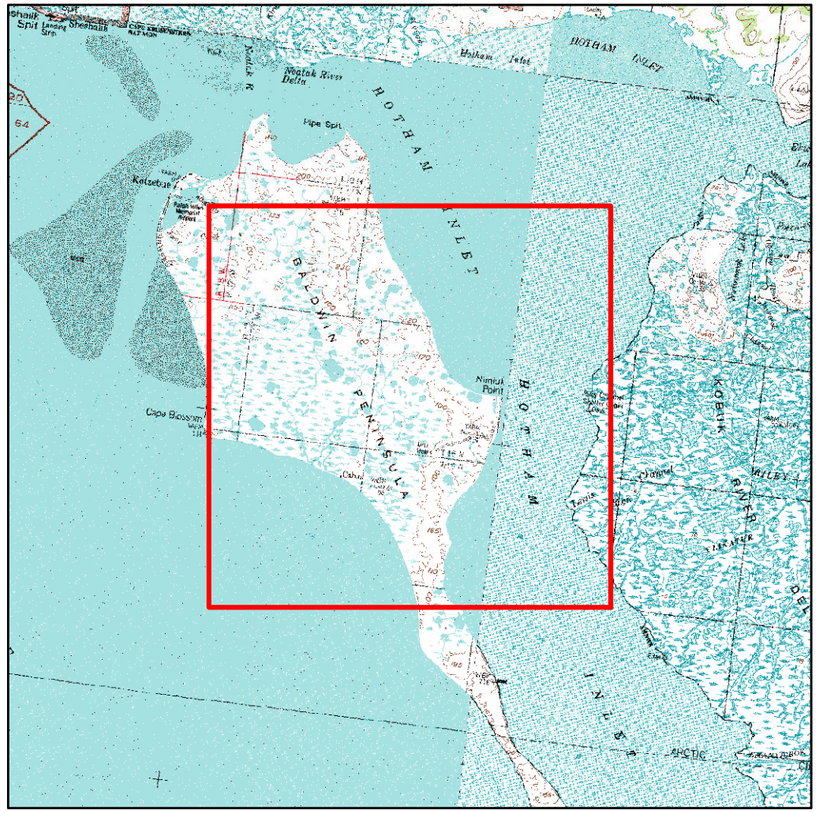

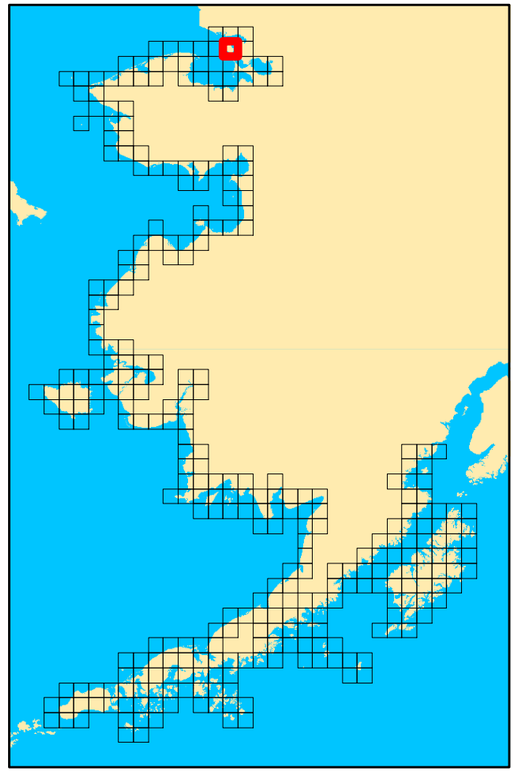

0 1 2 3 Km

Figure 13. Landsat trend analysis results for TM 1986–2001, tile AKH062V16. Significant near-infrared spectral change classified as land to water or water to land conversion.

Fig13_Results_TM_1986_2001_AKH062V16_Conversions_13-321.mxd 5/31/2013

AKH062V16: Landsat Trend Analysis Results, TM 2001–2011 (10 years with data)
Major Land Cover Conversions
Displayed over 2010 Imagery

1=Land to Water

2=Water to Land

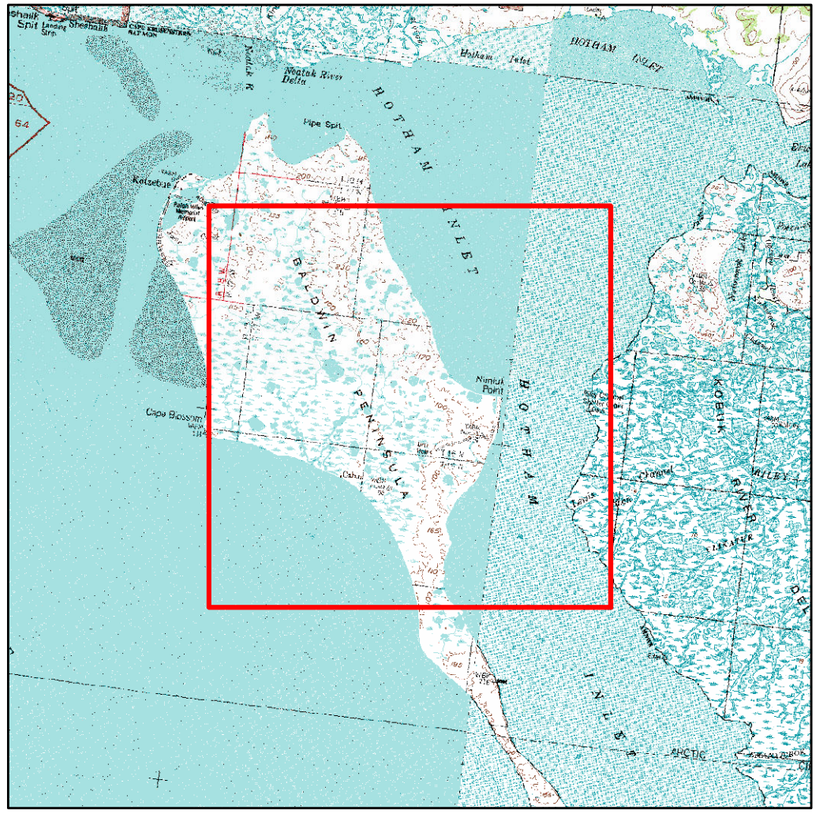

0 1 2 3 Km

Figure 14. Landsat trend analysis results for TM 2001–2011, tile AKH062V16. Significant near-infrared spectral change classified as land to water or water to land conversion.

Fig14_Results_TM_2001_2011_AKH062V16_Conversions_13-321.mxd 5/31/2013

AKH062V16: Landsat Trend Analysis Results, TM 1986–2011 (15 years with data)
Major Land Cover Conversions
Displayed over 2010 Imagery

1=Land to Water

2=Water to Land

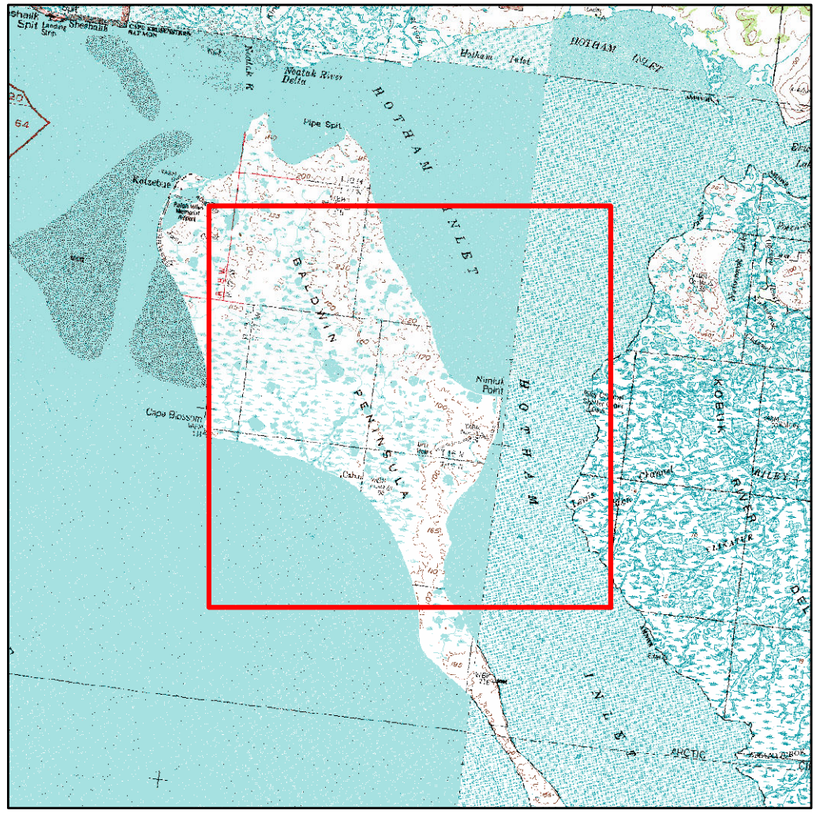

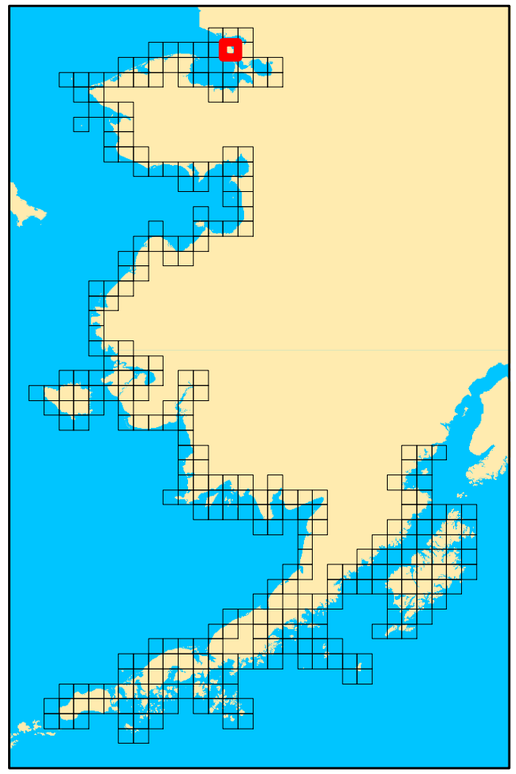

0 1 2 3 Km

Figure 15. Landsat trend analysis results for TM 1986–2011, tile AKH062V16. Significant near-infrared spectral change classified as land to water or water to land conversion.

Fig15_Results_TM_1986_2011_AKH062V16_Conversions_13-321.mxd 5/31/2013

AKH062V16: Landsat Trend Analysis Results,
41-year Time Series with 20-year Gap
(18 years with data)
MSS 1972–1979 and TM 1999–2011
Major Land Cover Conversions
Displayed over 2010 Imagery

1=Land to Water

2=Water to Land

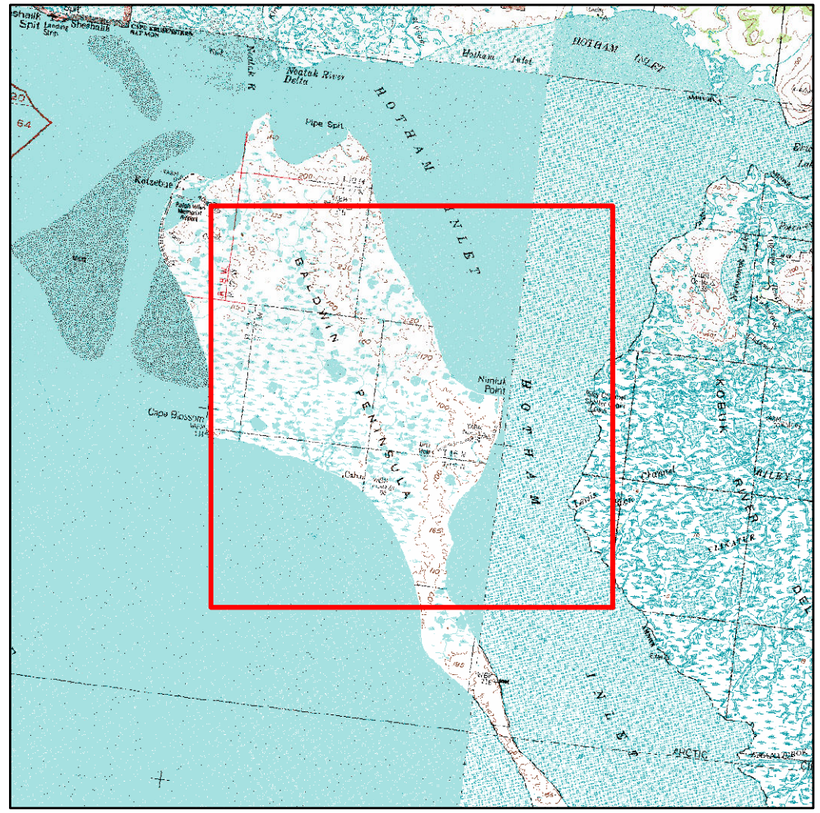

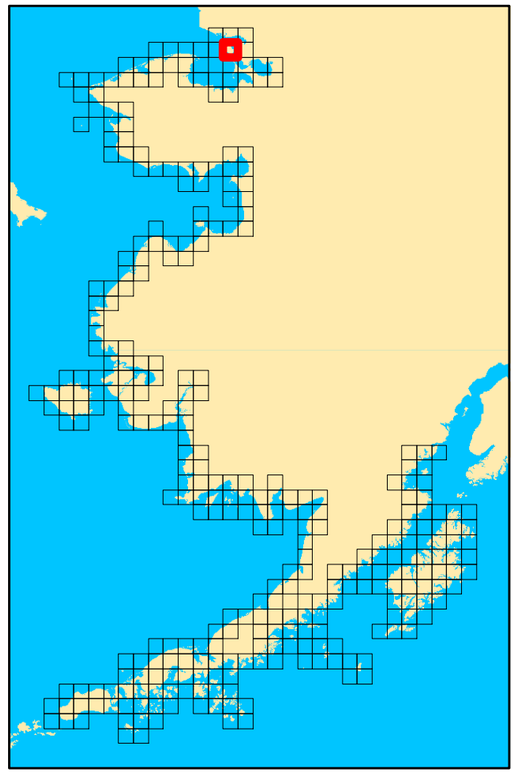

0 1 2 3 Km

Figure 16. Landsat trend analysis results for 41-year time series with 20 year gap: MSS 1972–1979 and TM 1999–2011, tile AKH062V16. Significant near-infrared spectral change classified as land to water or water to land conversion.

Fig16_Results_Gap_MSS_1972_1979_TM_1999_2011_AKH062V16_Conversions_13-321.mxd 5/31/2013

CONCLUSIONS

Availability of Landsat imagery for 1972–2011 was assessed for the coastal portion of the WALCC. Using conservative criteria selecting July–September scenes with cloud cover <= 20%,there was good coverage north of the Yukon-Kuskokwim Delta, sparser coverage for the Yukon-Kuskokwim Delta, Bristol Bay and the Alaska Peninsula, and moderate coverage for Kodiak Island and adjacent mainland (Figure 2). Temporally, coverage from the MSS sensor was high during the 1970s and TM/ETM+ coverage was high following the launch of Landsat 7 in 1999. Coverage during the 1980s and 1990s was patchy, with large expanses of the YK Delta and Alaska Peninsula having coverage from two or fewer scenes during particular eras.

Using a more liberal and less biased weighted cloud-free area approach and extending the seasonal range to include June, robust imagery coverage with six or more scenes per era is available across the entire study area during two eras of the 1970s and 2000s. There are areas with sparser data for the 1980s and 1990s, particularly for the period 1987–1998 (Figure 3).

Examples of the change detection methods using MSS imagery and TM/ETM+ imagery were provided for two tiles in the northern portion of the WALCC. A near-infrared reflectance metric was selected for the example analyses because it is available for both MSS and TM/ETM+ imagery and it minimizes atmospheric effects and noise (compared to metrics that use more than one band of the noisy MSS data).

Areas of significant spectral change were widespread. Increased NIR could be associated with conversion of water to land, or it could be recovery of vegetation from disturbance, shrubbification, phenology artifacts, or minor changes in sensor response across the time series. For the example analysis, a simple algorithm was developed to identify land to water and water to land transitions. Extensive coastal erosion and some accretion areas were identified over the full 39-year time series. Natural and human-caused coastal processes on river deltas and lagoons were also identified, along with (mostly non-coastal) lake drainage events.

Additional work on optimizing the change detection and classification would occur in Phase 2 and would focus on a) issues related to the resolution difference between MSS and TM/ETM+ (perhaps aggregating the TM/ETM+ rather than super-sampling the MSS); b) evaluation of

different statistical methods and classification methods to analyze and summarize the results. During the algorithm refinement stage it would make sense to focus on areas with existing, intensive and spatially explicit coastal erosion records—for example, the coast of Bering Land Bridge National Preserve (Manley 2012) and portions of the Yukon-Kuskokwim Delta.

Additional spectral metrics will be assessed for the full analysis, particularly for the TM/ETM+ portion of the time series (1985–present). NDVI and short-wave infrared reflectance are examples of the other spectral metrics. An advantage of using NDVI is that transitions between barren and vegetated land could be detected, though phenology variations and noisy MSS channels would complicate interpretation. The vegetation/soil transition is expected to be especially important in areas with extensive low-relief tidal flats, such as the Yukon-Kuskokwim Delta. Short-wave infrared reflectance has excellent land/water discrimination and has been used in a Landsat analysis of lake drainage in the Arctic Network of National Parks (Swanson 2013).

Assessments of the change detection approach over shorter time scales (10–25 years) identified changes that were in some cases consistent and in other cases were different from the results of the full 39-year time series analysis. Results from decadal scales can readily be computed and summarized; however, it will be challenging to discriminate real decadal changes from artifacts related to interannual variation and noise over the shorter time periods.

Another assessment of the change detection approach was conducted using a 39-year time series with a 20-year gap (representing the typical time series available for much of the Yukon-Kuskokwim Delta and Alaska Peninsula). The consistent results between analyses using the full 39-year time series and the 39-year time series with a 20-year gap provide good evidence that the change detection technique can be applied as long as good data are available for multiple years at the start and end of the time period.

The assessment of available imagery using a weighted cloud-free area approach showed that all portions of the WALCC have good data availability during the 1970s and from 1999–present. Some areas also had substantial imagery available in the 1980s and 1990s. The example time series analysis showed that the proposed change detection approach worked with both a full 39-year time series and for a 39-year time series with a 20-year gap. Therefore, we suggest that the Phase 2 analysis can proceed as proposed for the full coastline of the WALCC.

REFERENCES

Crist, E. P. and R. C. Cicone. 1984. A physically-based transformation of Thematic Mapper data—the TM Tasseled Cap. IEEE Transactions on Geoscience and Remote Sensing, GE-22: 256–263.

Fraser, R.H., I. Olthof, M. Carriere, A. Deschamps, and D. Pouliot. 2011. Detecting long-term changes to vegetation in northern Canada using the Landsat satellite image archive. Environmental Research Letters 6:1–9.

Kennedy, R. E., Z. Yang, and W. B. Cohen. 2010. Detecting trends in forest disturbance and recovery using yearly Landsat time series: 1. LandTrendr—temporal segmentation algorithms. Remote Sensing of Environment, 114: 2897–2910.

Macander, M.J., P.F. Miller, and M.T. Jorgenson. 2011. Time series data compilation and spectral change detection for the Teshekpuk Lake region. Unpublished report prepared by ABR, Inc.—Environmental Research & Services, Fairbanks, AK for Alaska Science Center, USGS, Anchorage, AK. 61 pp.

Manley, W. F., and L. R. Lestak. 2012. Protocol for high-resolution geospatial analysis of coastal change in the Arctic Network of Parks. Natural Resource Report NPS/ARCN/NRR—2012/537. National Park Service, Fort Collins, Colorado.

Masek, J. G., E. F. Vermote, N. E. Saleous, R. Wolfe, F. G. Hall, F. Huemmrich, F. Gao, J. Kutler, and T. K. Lim. 2006. A Landsat surface reflectance data set for North America, 1990-2000, IEEE Geoscience and Remote Sensing Letters, 3 (1): 69–72.

Swanson, D. K. 2013. Surface water area change in the Arctic Network of National Parks, Alaska, 1985-2011: analysis of Landsat data. Natural Resource Data Series NPS/ARCN/NRDS—2013/445. National Park Service, Fort Collins, Colorado.